# Molecular Dynamics Investigation of Relaxations in Zeolite ZSM-5 Based Amorphous Material

**ARTICLE** *in* THE JOURNAL OF PHYSICAL CHEMISTRY B · SEPTEMBER 2004

Impact Factor: 3.3 · DOI: 10.1021/jp0474778



**3 AUTHORS**, INCLUDING:

C. Oligschleger
Hochschule Bonn-Rhein-Sieg
**30** PUBLICATIONS **683** CITATIONS

# Molecular Dynamics Investigation of Relaxations in Zeolite ZSM-5 Based Amorphous Material

**A. B. Mukhopadhyay,*,† C. Oligschleger,‡ and M. Dolg†**

*Institut für Theoretische Chemie, Universität zu Köln, Greinstr. 4, D-50939 Köln, Germany, and Fachhochschule Bonn-Rhein-Sieg, University of Applied Sciences, von-Liebig-Str. 20, D-53359 Rheinbach, Germany*

*Received: June 11, 2004; In Final Form: August 5, 2004*

We present results from molecular dynamics computer simulations of the dynamic properties of amorphous material derived from zeolite ZSM-5, in particular secondary relaxations for temperatures below the critical temperature. We observe local jumps where groups of atoms move collectively. At low temperatures the relaxations comprise mainly of one-dimensional chains of atoms. The dimensionality of the relaxing centers increases with the temperature due to side branching. Both the displacement vector and the number of atoms participating in the jumps increase with temperature. The possibility of having reversible jumps decreases with increasing temperature due to a strong drop in the potential energy during aging. There exist very prominent peaks in the van Hove correlation functions as a manifestation of the hopping processes. The dynamics of the oxygen atoms is found to be more heterogeneous than those of the silicon atoms.

## 1. Introduction

Amorphous phases exhibit over an extremely broad range of time particular motional processes known as relaxations.[1−4] Primary or α relaxations are related to flow processes, and the relaxation times follow the Vogel−Fulcher−Tammann equation.[5,6] In contrast, the secondary or $\beta$ relaxations are envisaged as thermally activated transitions over the barriers separating the local minima in the potential energy landscape[7−9] and follow an Arrhenius relation with respect to the relaxation time.[10] Thus, an insight into the topography of the inherent structures can be obtained by investigating these relaxations.[11−13] The mode coupling theory predicts the existence of a critical temperature $T_c$, at which the relaxation dynamics of the system changes qualitatively.[14] The α processes become frozen below $T_c$, while the $\beta$ relaxations persist also below this temperature; however, because of the slowing down of the dynamics, their importance decreases with decreasing temperature.[15]

In recent years one particular aim of intensive experimental and theoretical studies of relaxations in amorphous solids and liquids was to determine whether the relaxations involve only groups of atoms or they are spread over the whole system.[16−19] While the first case is related to the heterogeneous scenario, the latter features are homogeneous ones. Various investigations showed that the system becomes homogeneous at high temperatures for sufficiently long times, corresponding to the α relaxation regime.[20,21] In the intermediate time domain, corresponding to the $\beta$ relaxations, the heterogeneity becomes more pronounced when the system is cooled.[22]

The local relaxations can be perceived as changes in the configurations by thermally activated hopping of some groups of atoms over barriers. The soft potential model predicts that these local relaxations at low temperatures are strongly correlated with the local soft vibrations.[23] By fitting this model to the experimental data, one finds effective masses of 20−100 atomic masses for the entities moving in the effective soft potential.[24,25] Investigations of the relaxations in various systems like metallic glasses also proved the existence of strong cooperative motions consisting of chains of atoms.[26−28]

Recently, we have performed detailed molecular dynamics (MD) based theoretical investigations of structural and vibrational properties of partially amorphized structures derived from zeolite ZSM-5.[29−31] In addition, quantum chemical methods were applied to study special structural features occurring in these simulations, i.e., edge-connected $SiO_4$-tetrahedra.[32] In this final contribution on our chosen model system we present a MD investigation of secondary relaxations occurring in these materials at the low-temperature regime (below $T_c$). The occurrence of these relaxations might change the level of crystallinity, and hence, it can affect the selectivity of the reactions which are dependent on the percentage of crystallinity.[33] The dynamics show some interesting phenomena like aging and dynamical heterogeneities at the intermediate time scales studied (1 ps to 0.6 ns). In section 2, we describe the computational details. The time evolution on the energy landscape, the structures of relaxations, the correlations between the jumps, and the heterogeneity of relaxations are discussed in section 3. Some concluding remarks are added at the end.

## 2. Computational Details

The methodology of the MD simulation and the generation of the amorphous structures have been described in detail in our recent works.[29,30] The interaction potentials used in our simulation were obtained from the literature.[34] The system consists of 3456 atoms whose initial coordinates corresponding to the orthorhombic ZSM-5 crystal modification were taken from the literature.[35] The mass density in the simulation cell was kept constant at the corresponding experimental mass density 1.785 g/cm$^3$ of (crystalline) ZSM-5 at normal pressure[35]

† Universität zu Köln.
‡ University of Applied Sciences.
* Corresponding author. Present address: Department of Physics and Astronomy, Michigan State University, East Lansing, MI 48824. E-mail: mukhopad@pa.msu.edu.

10.1021/jp0474778 CCC: $27.50 
Published on Web 09/22/2004

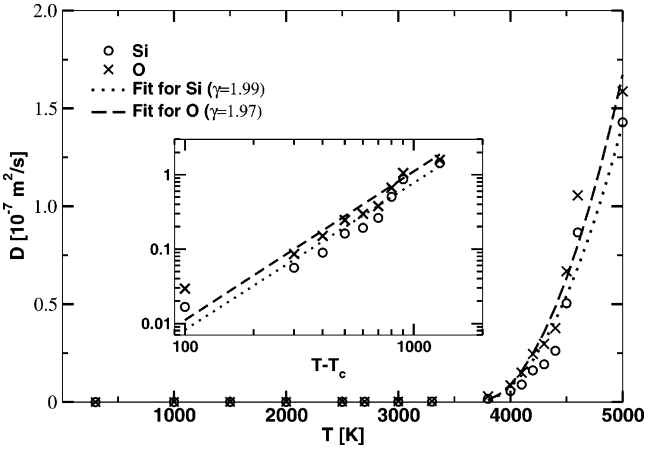


**Figure 1.** Element-specific diffusion constants in zeolite ZSM-5 based partially amorphized material (starting average PEC of 60%) at different temperatures. Dotted and dashed lines are the results of a fit to the high-temperature data for Si and O, respectively, with the fractional power law $D \propto (T - T_c)^{\gamma}$ with a critical temperature of 3700 K. The inset represents $D$ of Si and O vs $T - T_c$ in the log−log representation.

during all MD runs. To obtain structures corresponding to different extents of amorphization, the initial structure was heated to different maximum temperatures followed by rapid quenching to 300 K (with a heating rate of $R_{heat} = 4.7 \times 10^{12}$ K/s and a quenching rate of $R_{quench} = 4.7 \times 10^{12}$ K/s).

We choose a semiquantitative description to analyze the extent of amorphization, which is similar to the percentage of XRD crystallinity advocated by Nicolaides.[33] The extent of amorphization is quantified as the "percentage of energy crystallinity" (PEC)[29] which is defined as

$$\mathrm{PEC} = \frac{E_{\mathrm{amorphous}} - E_{\mathrm{configuration}}}{E_{\mathrm{amorphous}} - E_{\mathrm{crystalline}}} \times 100 \qquad (1)$$

Here $E_{amorphous}$ corresponds to the energy per atom of the maximum amorphized structure that we have obtained after minimization in our simulations, i.e., −16.90 eV/atom (in the configurational space spanned in our simulations no higher lying minimum occurred). $E_{crystalline}$ represents the energy per atom of the crystalline ZSM-5 system, i.e., −17.17 eV/atom, and $E_{configuration}$ stands for the energy of the structure, whose PEC we are interested in. Note that our definition of PEC depend via $E_{amorphous}$ on all parameters determining heating, equilibration, and the quenching process, i.e., the maximum temperature and the equilibration time at the maximum temperature as well as the quenching rate. The temperature control was performed via the velocity rescaling method. Each time step corresponds to 2 fs and was kept sufficiently small in order to have a negligible drift in energy. In all 20 systems were chosen to study the relaxational dynamics below $T_c$.

An estimate of $T_c$ (as given in refs 21 and 36) is usually obtained from the diffusion constant $D$ of the system calculated as a function of temperature using the relation

$$D_{\alpha} = \lim_{t \to \infty} \frac{1}{6t} \langle |\boldsymbol{R}_{\alpha}(0) - \boldsymbol{R}_{\alpha}(t)|^2 \rangle \qquad (2)$$

Here $\boldsymbol{R}_{\alpha}(t)$ is the time-dependent position vector of a particle of type $\alpha \in \{\mathrm{Si,O}\}$ and $\langle ... \rangle$ denotes the configurational average. According to the mode coupling theory, the temperature dependence of the diffusion is given by a power law, i.e., $D \propto (T - T_c)^{\gamma}$, where $\gamma$ is the critical exponent. In Figure 1, we present the dependence of $D$ with respect to $T$. A fit to the high-temperature data yielded a $T_c$ of 3700 K with $\gamma$ values of 1.99 and 1.97 for Si and O, respectively. For viscous silica, a MD simulation gave the values $T_c = 3330$ K, $\gamma(\mathrm{Si}) = 2.15$, and $\gamma(\mathrm{O}) = 2.05$.[22] After the MD quench to 300 K as described above, the chosen structures were heated to elevated temperatures (300 → 1000 → 2000 → 3000 K) and further aged at each temperature for 300 000 time steps corresponding to 0.6 ns. All equilibrations were done via constant-temperature MD simulations. The average pressure in the system were 0.1451, 0.1447, 0.1440, and 0.1439 GPa at 300, 1000, 2000, and 3000 K, respectively, with a maximum deviation of ±4% occurring at 3000 K. To detect relaxations at a given temperature in the course of MD runs, we monitored the atomic displacements defined as

$$\Delta R(t) = \sqrt{\sum_k [\mathbf{R}_k(t) - \mathbf{R}_k(0)]^2} \qquad (3)$$

Here $\mathbf{R}_k(t)$ is the position vector of the particle $k$ at time $t$, whereas $\mathbf{R}_k(0)$ is the one at the starting or reference configuration on the potential energy surface. If the total displacement of the atoms exceeds a cutoff value and the residence time of the atoms in the new positions also exceeds a minimal period of at least 3 times the period of a typical soft vibrational mode, the new positions of the particles were accepted as a starting point for the determination of a possible new minimum configuration. All the stored coordinates were then quenched to $T = 0$ K using a combined steepest-descent-conjugate-gradient (SDCG) algorithm[37] to locate the nearest minimum configuration in the potential energy surface. In the following section we discuss the relaxation properties of these minimum structures during aging at the temperatures mentioned above.

## 3. Results and Discussion

**3.1. Time Evolution on the Energy Landscape.** Quenching the positions of the stored configurations to $T = 0$ K, the configurations of the underlying minima can be found. Similar to the above definition of the atomic displacement during the MD run, one can define $\Delta R^0(t)$ for the actual minima obtained by the combined SDCG algorithm as

$$\Delta R^0(t) = \sqrt{\sum_k [\mathbf{R}_k^0(t) - \mathbf{R}_k^0(0)]^2} \qquad (4)$$

$$= \sqrt{\sum_k (\Delta R_k^0)^2} \qquad (5)$$

where $\mathbf{R}_k^0(t)$ is the time-dependent position of the particle $k$. The superscript "0" refers to the values corresponding to the minima on the potential energy surface ($T = 0$ K). Similarly, one can define $E°(t)$ as the minimum energy obtained by the combined SDCG algorithm.

We did not observe any major relaxation accompanied by large energy reduction or sharpening of pair distribution functions, which are often an indication of crystallization of the configuration.[11] Figure 2a,b shows the time evolution of the ensemble averaged potential energies and displacements per atom obtained during the aging of the systems at different temperatures. These averages were taken over 10 configurations with a starting average PEC of 60%. In general, the potential energy drops during aging. After heating there is a subsequent leveling off of the potential energy at lower temperatures (300 and 1000 K). The largest part of the atomic displacement immediately follows after heating. The average displacements of the atoms is very small, i.e., less than 2% of the Si−O bond

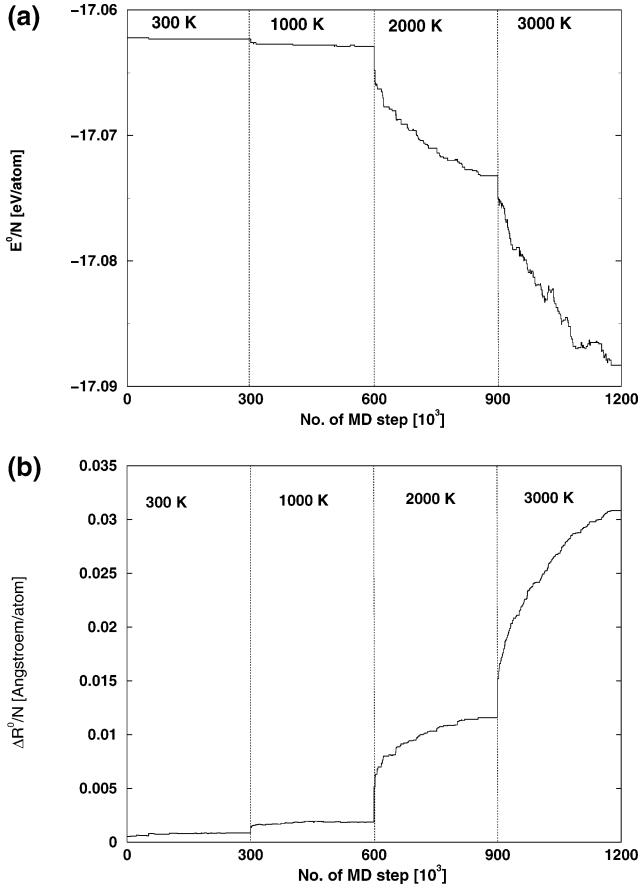


**Figure 2.** (a) Changes in the potential energy per atom and (b) displacement per atom during aging obtained as ensemble averages. The temperature intervals are indicated by the dotted lines. The heating procedures consisting of 50 000 MD steps between each temperature interval are omitted in the plots.

distance at 3000 K. The decrease in the average potential energy and displacement per atom increases with temperature as the possibility to cross large energy barriers and to visit farther away minima in potential energy landscape increases.

**3.2. Structure and Mode of Relaxations.** To study the localization behavior of the relaxations, we calculated analogous to our study of the vibrations[30] the relaxational effective mass and participation ratio. The effective mass of a relaxation is defined as

$$M_{\text{eff}} = m_{\max} \frac{(\Delta R^0)^2}{|(\Delta \mathbf{R}^0_{\max})^2|} \tag{6}$$

where $\Delta R^0$ represents the distance between two successive minimum configurations as obtained using eq 5. $|\Delta(\mathbf{R}^0_{\max})^2|$ and $m_{\max}$ denote the maximal distance and mass of the farthest jumping atom. The participation ratio is defined as

$$P_{\Delta R^0} = \frac{(\Delta R^0)^4}{N\sum_k (\mathbf{R}_k^{\text{i},0} - \mathbf{R}_k^{\text{f},0})^4} \tag{7}$$

where $\mathbf{R}_k^{\text{i},0}$ and $\mathbf{R}_k^{\text{f},0}$ denote the initial and the final position of the atom $k$ and $N$ represents the total number of atoms. The participation ratio has the value $n/N$ if $n$ atoms are equally involved in the relaxation process. If all atoms contribute equally in the jump, the resulting participation ratio will be 1.

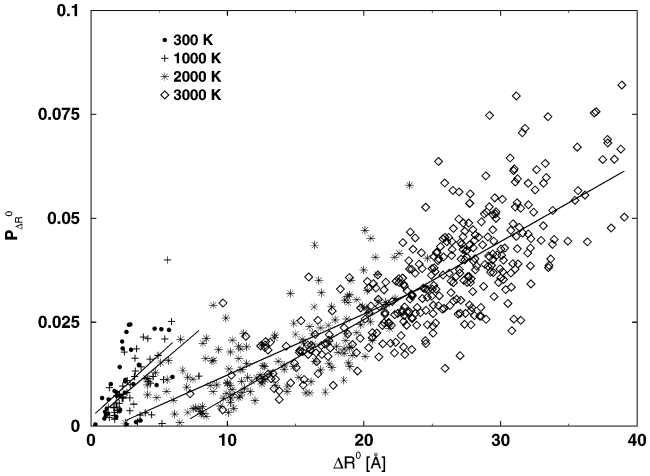


**Figure 3.** Participation ratios of relaxations against jump distance at different temperatures. The linear least-squares fits to the points corresponding to different temperatures are shown. The slopes of the lines are 0.003027894, 0.002808881, 0.00146869, and 0.001873854 $\text{Å}^{-1}$ at temperatures 300, 1000, 2000, and 3000 K, respectively. The number of jumps shown here is 45, 50, 158, and 339 at 300, 1000, 2000, and 3000 K, respectively.

The influence of the temperature on the jump lengths and the participation ratios are shown in Figure 3. The participation ratios roughly grow linearly with the jump lengths. The average participation ratios of 0.009, 0.010, 0.018, and 0.036 are observed for jumps at 300, 1000, 2000, and 3000 K, respectively. These correspond to the effective masses of 7, 10, 16, and 29 atoms, respectively.

To analyze the relaxation structures, we define a dimensionality of the relaxations and calculate for each jump $j$ the tensor $\mathbf{H}$

$$H_{\alpha\beta}(j) = \frac{\sum_k |\Delta \mathbf{R}_k^0(j)|^\mu (R^0_{\alpha,k} - R^{\text{c.m.}}_\alpha)(R^0_{\beta,k} - R^{\text{c.m.}}_\beta)}{\sum_k |\mathbf{R}_k^0(j)|^\mu} \tag{8}$$

where the exponents $\mu = 2$ and $\mu = 4$, corresponding to the effective mass and participation ratio, respectively. $\mathbf{R}^{\text{c.m.}}$ is the corresponding center-of-mass coordinate of the relaxation:

$$\mathbf{R}^{\text{c.m.}} = \frac{\sum_k |\Delta \mathbf{R}_k^0(j)|^\mu \mathbf{R}_k^0}{\sum_k |\Delta \mathbf{R}_k^0(j)|^\mu} \tag{9}$$

Diagonalizing $\mathbf{H}$, we obtain three eigenvalues $\rho^i(j,\mu)$ (for $i = 1, 2, 3$). From these an average radius of gyration is obtained as

$$R_{\text{gyr}}(j,\mu) = \sqrt{\frac{1}{3}\sum_i \rho^i(j,\mu)} \tag{10}$$

If a relaxation is localized on a single atom, $R_{\text{gyr}} = 0$. For an extended relaxation, it is the root-mean-square distance with the weight determined by $\mu$. An effective dimension of the relaxation can be defined as

$$d(j,\mu) = \sum_i \rho^i(j,\mu)/\max\, \rho^i(j,\mu) \tag{11}$$

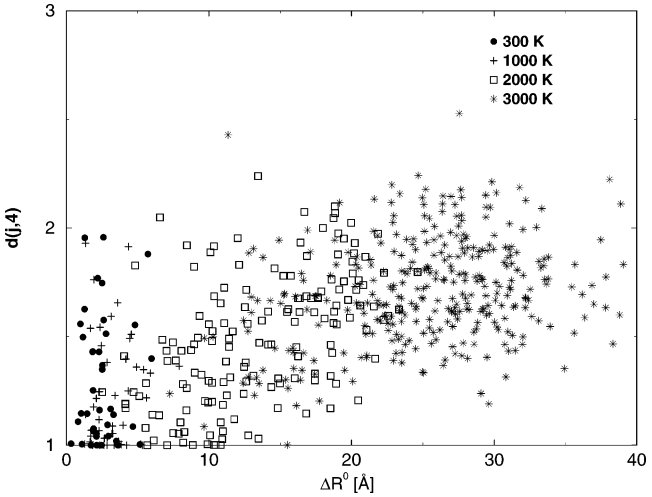


**Figure 4.** Dimensions of the jumps related to the participation ratio at different temperatures.

**TABLE 1: Average Dimensionalities $\bar{d}(\mu)$ and Average Radii of Gyration $R_{gyr}(\mu)$ (in Å) Are Summarized Corresponding to the Exponents $\mu = 2$ and $\mu = 4$**

| $T$, K | $\bar{d}(2)$ | $\bar{d}(4)$ | $\bar{R}_{gyr}(2)$ | $\bar{R}_{gyr}(4)$ |
|---|---|---|---|---|
| 300 | 1.34 | 1.22 | 6.10 | 3.88 |
| 1000 | 1.51 | 1.28 | 8.63 | 5.46 |
| 2000 | 1.55 | 1.48 | 11.29 | 8.69 |
| 3000 | 1.72 | 1.70 | 13.05 | 11.36 |

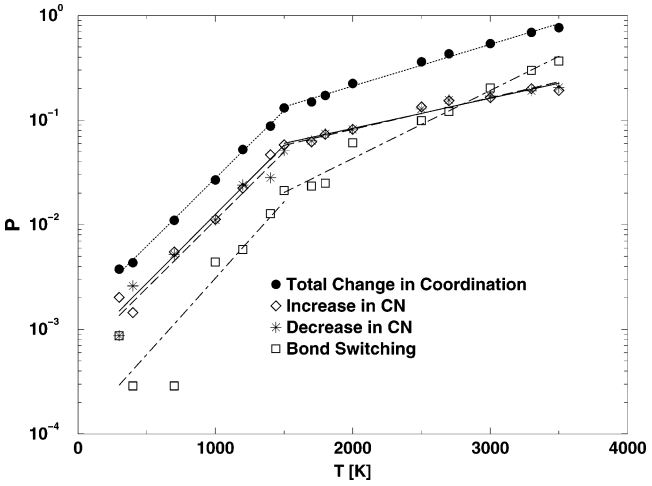


**Figure 5.** Fraction of atoms undergoing bond changes during relaxation at different temperatures. Dotted, solid, dashed, and dot−dashed lines represent least-squares fits for the total change in coordination, increase in CN, decrease in CN, and bond switching, respectively.

Figure 4 and Table 1 summarize the results for temperature-dependent dimensionalities and average radii of gyration, averaged over the whole relaxation. We find that at lower temperature the relaxations are of lower dimensionality. At elevated temperatures the average dimensionality as well the average gyration radius increases due to the side branching of the relaxing chains. The effective mass related values are always higher than the ones related to the participation ratio, reflecting the different weights of the long-range displacements.

Figure 5 summarizes the results of the relaxations with respect to the Si−O bond changes in terms of the increase or the decrease in the coordination number (CN) during relaxations at different temperatures observed for 0.6 ns. The cutoff value of the Si−O bond is 1.8 Å taken from the position of the minimum according to the most intense peak in the total pair distribution function (for details refer to ref 29). Another possibility may be that the CN is conserved, but the atoms change their coordination partner during the relaxation. We denote such changes as "bond switching" in Figure 5. For the total change in coordination, there exists a transition temperature at 1500 K, where the relative importance of the CN changes and bond switching changes significantly. At lower temperatures (below 1500 K) the relaxations are mainly due to the small changes in the atomic positions and bond breaking occurs for less than 10% of atoms. At elevated temperatures, bond formations and dissociations become very significant. The bond switching mechanism is not the dominating process at low temperatures. At 2000 K it becomes comparable to the other two possibilities (increase and decrease in the CN), and beyond 2800 K it is the bond switching scenario which dominates. Greaves and co-workers have studied rheology of collapsing zeolites (zeolite A and zeolite Y) by temperature and pressure.[38,39] They found that there exists another transition temperature $T_A$ referred to as temperature of collapse (well below the melting temperature), where the crystallinity (measured by XRD data) drops drastically. Experimentally, $T_A$ for zeolite A and zeolite Y are found to be 1173 and 1193 K, respectively. The temperature of collapse increases with the heating rate. Greaves et al. found amorphization accompanied by the reconfiguration of the network takes place around this temperature. We propose that the transition energy of 1500 K obtained in our simulation might correspond to the $T_A$ of the partially amorphized system. The bond dissociations and formations indicate the process of collapse of the network along with its reorganization. However, the analysis of the variation of $T_A$ with respect to the heating rate is not within the scope of this article.

To study the type of motions involved during the relaxations, we performed the projections of the relaxation vectors onto the symmetry modes of the ideal Si−O−Si ($C_{2v}$ symmetry) and $SiO_4$ ($T_d$ symmetry) subunits, analogous to the mode analysis for studying the vibrational properties.[30] The calculated contributions of the motion involved in the relaxations exhibited by the subunits are shown in Table 2. The respective motions of the oxygen and silicon atoms in the $SiO_4$ and Si−O−Si subunits mostly stem from rotation followed by bending. The contributions of the individual motions are quite stable over a large temperature range (300−3000 K) with a small exception. The contributions from the symmetric and antisymmetric stretching motions are not so significant. The rotational contribution of the Si−O−Si subunit decreases slightly with increasing temperature, whereas the bending contributions increases. Qualitatively, these contributions of relaxations are similar to that of vitreous silica glasses.[40] In these systems, both rotational and bending motions dominate the overall contributions. However, the simulation of vitreous silica showed that the antisymmetric stretching of both the structural units are also important and contributes to ≈20% of the total relaxation. We predict this difference to be due to the presence of floppy modes in these partially amorphized zeolitic systems, which are mainly rotational and bending in character.[31] According to the soft-sphere potential model, there exists a correlation between local relaxations and soft vibrations. In ref 31 we have investigated the contributions of the type of motions involved in the boson peak region in partially amorphized ZSM-5 systems. The contributions of Si−O−Si subunits and $SiO_4$ subunits listed in Table 2 are very similar to the modes corresponding to the boson peak region.[31] This may imply that these relaxations in part contribute to the boson peak.

**TABLE 2: Contributions (in percent) of the Relaxations Exhibited by Si−O−Si and $SiO_4$ Subunits by the Projectional Analysis in Structures with PEC of 60%[a]**

| | $SiO_4$ | | | | | Si−O−Si | | | |
|---|---|---|---|---|---|---|---|---|---|
| *T*, K | $S^{(A_1)}$ | $S^{(F_2)}$ | $B^{(F_2)}$ | $B^{(E)}$ | rot. | $S^{(A_1)}$ | $S^{(B_1)}$ | $B^{(A_1)}$ | rot. |
| 300 | 1 | 1 | 11 | 10 | 77 | 1 | 0 | 18 | 81 |
| 1000 | 0 | 0 | 9 | 14 | 77 | 0 | 0 | 17 | 83 |
| 2000 | 1 | 2 | 11 | 10 | 76 | 1 | 1 | 20 | 78 |
| 3000 | 1 | 3 | 11 | 9 | 76 | 2 | 1 | 21 | 76 |

[a] "S", "B", and "rot." represent the stretching, bending, and rotational contributions, respectively, and the superscripts denote the symmetry of the motions, in the subunit point groups $C_{2v}$ (Si−O−Si) and $T_d$ ($SiO_4$).

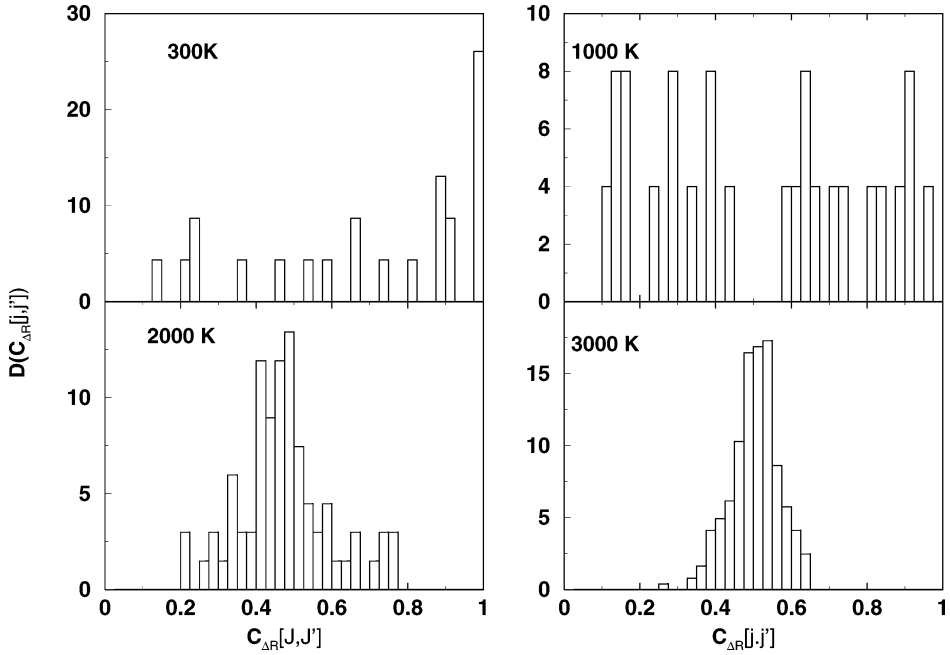


**Figure 6.** Distribution of correlations between successive jumps (in percent) at different temperatures. The numbers of successive jumps considered here are 23, 25, 68, and 243 at 300, 1000, 2000, and 3000 K, respectively.

**3.3. Correlation between Jumps.** Looking more closely at the active atoms, the relaxations are found to consist of collective jumps of chains of atoms. These jumps are not uncorrelated events, but successive jumps tend to involve the same atoms. As a quantitative measure, we calculate the correlation between the jumps as

$$c_{\Delta R^0}[j, j'] = \frac{\sum_k \Delta R_k^0[j] \Delta R_k^0[j']}{\Delta R^0[j]\ \Delta R^0[j']} \qquad (12)$$

where $j$ and $j'$ denote successive relaxations. For reversible jumps, $c_{\Delta R^0}[j, j']$ is unity, and for completely uncorrelated jumps one would get values of the order of $1/N$.

Figure 6 shows the observed distributions of all the correlation values averaged over all the relaxations. At low temperatures (300 and 1000 K) there exists a wide distribution of the correlations. Extremely high-correlated jumps are mainly due to reversible jumps, whereas very low-correlated ones imply that different active regions of the system contribute to the relaxations at different times. (Only a few atoms relax at different places and at different times.) In contrast, at high temperatures (2000 and 3000 K), the jumps with very high and very low correlations become rare. The former case is due to a strong drop in the potential energy, and hence, the possibility of having reversible jumps or highly correlated successive jumps is removed. The latter case is due to the aggregation of different active regions to form large complexes. Such aggregation causes an increase in the size of the relaxing center (cf. increase in $\bar{R}_{gyr}$ and participation ratios in the previous section) which relaxes all together at the same time and thus decreases the possibility of jumps with very low correlations. Similar correlation studies on relaxations were performed by Oligschleger[40] on vitreous silica. Calculation of the correlation between successive jumps at temperatures 270, 870, and 1670 K gave values of 0.585 ± 0.314, 0.654 ± 0.089, and 0.666 ± 0.082, respectively. Despite the difference between the absolute value of the correlations obtained in our simulation on partially amorphized ZSM-5 and that provided in ref 40 on vitreous silica, the natures of these correlations are very similar. Both simulations reveal that at very low temperature several active regions coupled via a few atoms contribute to the jumps. At higher temperatures these local regions aggregate to a larger complex.

**3.4. Heterogeneity.** A detailed picture about the atomic motions in the relaxations can be obtained by investigating the self-part of the van Hove correlation function (VHF) for atoms of type α, $G_s^\alpha(R,t)$, defined as

$$G_s^\alpha(R,t) = \left\langle \frac{1}{N_\alpha} \sum_{i=1}^{N_\alpha} \delta(R - |\mathbf{R}_i(t) - \mathbf{R}_i(0)|) \right\rangle \qquad (13)$$

$\mathbf{R}_i(t)$ is the time-dependent position vector of atom $i$, and $\mathbf{R}_i(0)$ corresponds to the initial configuration. If all the atoms have the same mobility, the VHF is a Gaussian one with respect to $R$ for a given time. However, if atoms are trapped in cages or

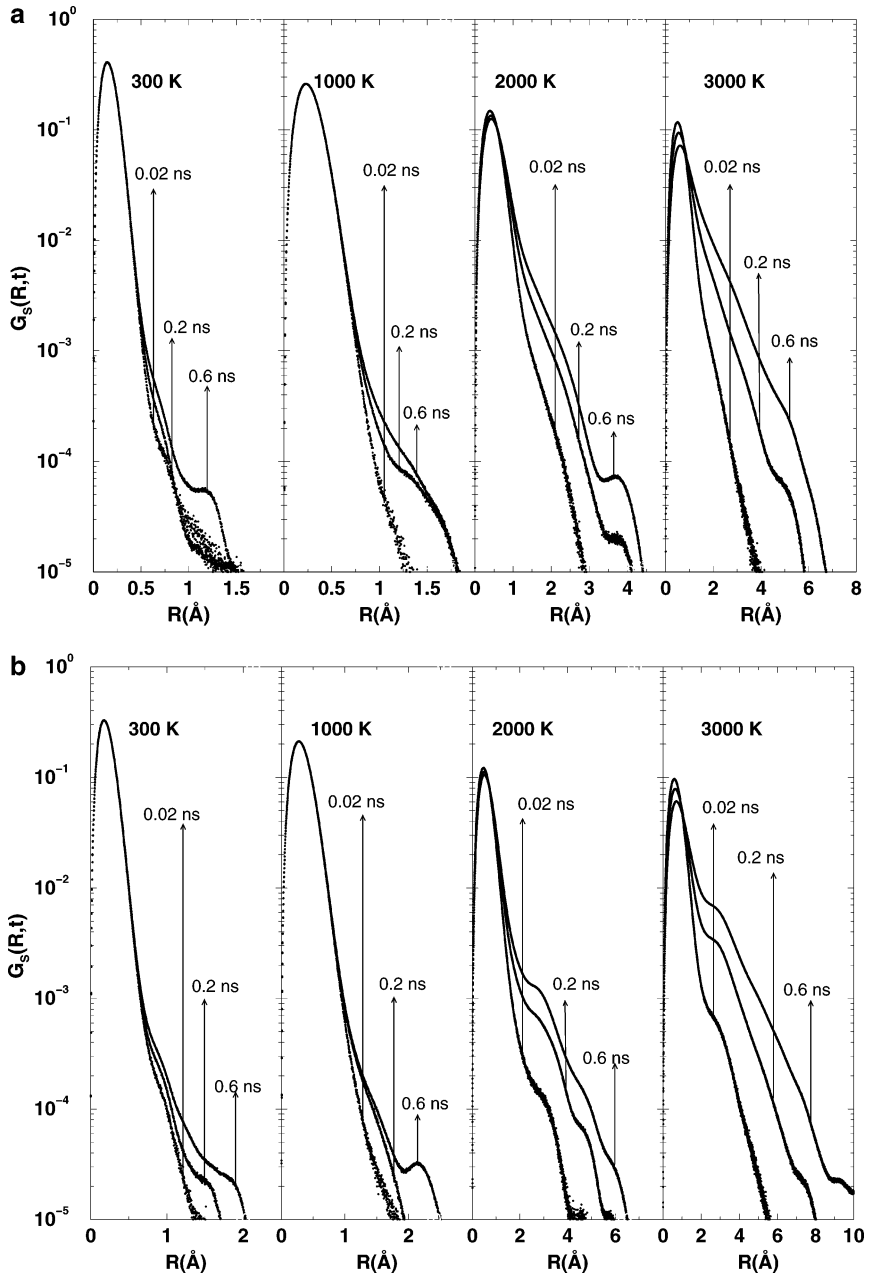


**Figure 7.** Log−linear plots of the time-dependent VHFs of (a) Si and (b) O atoms at different temperatures.

some are more mobile than the rest, the resulting function will be a non-Gaussian one.

In Figure 7, we show the time-dependent element-specific VHFs at 300, 1000, 2000, and 3000 K and at times 0.02, 0.2, and 0.6 ns. We observe that with increasing temperature the atoms move over larger distances as the particles have greater kinetic energy. A striking feature is the occurrence of peaks and shoulders in these correlation functions, which is a direct evidence of hopping processes existing in the system. Since at low temperatures (300 and 1000 K) the bond breaking and bond formation processes are rare (cf. Figure 5), the shoulders and the peaks are entirely due to the internal motions of the atoms in the subunits. A distinct peak occurs at 2.2 Å for the VHFs of the oxygen atoms at 1000 K. This position corresponds to the first (small) peak in the O−O pair-distribution function related to the edge-sharing tetrahedral units (refer to ref 29 for details on structural properties). We propose these jumps can be considered as the rotational motion of bridged oxygen atoms belonging to 2-fold rings. At higher temperatures (2000 and 3000 K) the bond breaking and formation processes (along with the bond switching processes) become quite prominent, and hence, large distant hopping associated with defects or defect formation becomes significant. These processes show important implications on the VHFs, which are very prominent at 2000 K. There exist shoulders at 2.6 and 5.0 Å in the VHFs of oxygen, whose positions correspond to the first (sharp and distinct) and second peak in the O−O pair distribution function. There also exist distinct peaks at 4.0 Å in the VHFs of silicon, whose positions can be related to the second peak in the Si−O pair distribution function. These jumps can be envisaged as the combined effects of defects corresponding to the 1-fold or the 3-fold coordinated oxygen atoms along with the modification of the framework structure. The former effect is also seen in viscous silica melt at 2750 K as investigated by Horbach and Kob.[22] The latter effect (not observed in viscous silica[22]) can be related to the formation or collapse of the ring structure present in these partially amorphized zeolitic systems. We also observe this phenomenon in the analysis of ring size distribution

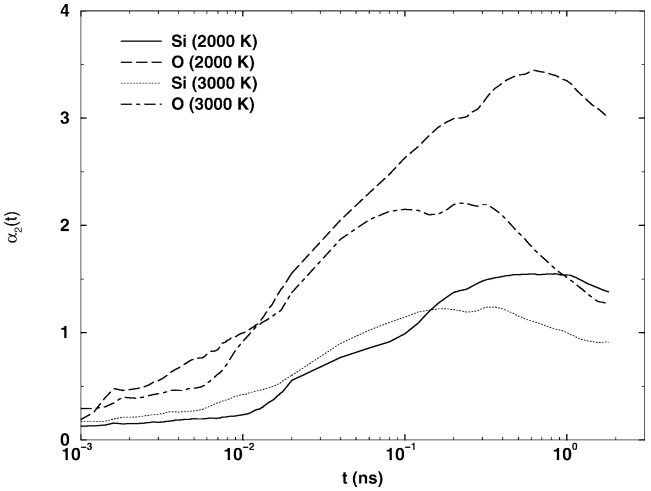


**Figure 8.** Log−linear plot of the non-Gaussianity parameter for Si and O at 2000 and 3000 K.

during an amorphization of zeolites as investigated in ref 29. The analysis of CN showed a presence of a transition temperature $T_A = 1500$ K, where a significant difference occurs in the behavior of the bonding situation. We suggest that at this temperature the reorganization of the network begins. One also observes crowding of the graphs at lower temperatures compared to the ones observed at 3000 K along with broadening of the VHFs at 3000 K. The former observations provide evidence for the manifestation of the cage effect. At lower temperatures the particles are unable to leave the cage formed by other particles that surround them over the time scale studied in this simulation. However, at higher temperatures the particles have sufficient kinetic energy to overcome this confinement; hence, the motion starts to get more diffusional in nature.

The non-Gaussianity parameter (NGP)

$$\alpha_2(t) = (3/5)\langle R^4(t)\rangle/\langle R^2(t)\rangle - 1 \qquad (14)$$

quantifies the deviation of $G_s(R,t)$ from a Gaussian form. Figure 8 shows in a log−linear plot $\alpha_2$ at 2000 and 3000 K covering a span of 3 orders of magnitude in $t$. At very short times the NGP is quite small and limiting to zero. In the intermediate time range (0.01−1.00 ns) the NGP increases with time and exhibits a maximum. The limiting behavior at large times is more difficult to compute, especially at the low temperature. The limiting behavior for large times has been studied for various other systems, and usually the NGP tends to zero.[21,41,42] For sufficiently long times the non-Gaussianity becomes more pronounced for lower temperature (2000 K) than higher one (3000 K) for both Si and O atoms. The value of the maximum scales by a factor of ≈1.5 with respect to the temperature. The positions of the maxima for both Si and O shifts by half an order of magnitude of $t$ by decreasing the temperature from 3000 to 2000 K. These observations suggest that at below $T_c$, the non-Gaussianity which is prevalent at the intermediate time scale becomes more pronounced as the temperature is reduced. The general features about the non-Gaussianity outlined here are also similar to the ones observed for an amorphous selenium system below the critical temperature.[21] Our work demonstrates that these features also persist for a completely different system. At both temperatures the oxygen atoms have a higher value of NGP; hence, there is clear evidence that the oxygen atoms probe a more heterogeneous environment than the silicon atoms, which can be attributed to their smaller mass.

## 4. Conclusion

In our present work we have investigated the relaxational properties of zeolite ZSM-5 based amorphous material. The study was restricted to the secondary processes at temperatures corresponding to 300, 1000, 2000, and 3000 K. The partially amorphized structures were obtained by quenching configurations, which were generated by heating the ZSM-5 crystalline structure using a molecular dynamics simulation.

At higher temperatures (2000 and 3000 K), the configurations show a sharp drop in the potential energies during aging and reflecting the possibility to visit farther away minima increases. At low temperatures (300 and 1000 K), the relaxations are mainly due to the small changes in the positions of the atoms. Bond creations and annihilations become significant at higher temperatures (2000 and 3000 K). Analysis of coordination numbers with respect to the temperature shows a transition temperature at 1500 K, which can be considered as temperature of collapse. We predict that reconfiguration of the network starts at this temperature. The localization of the relaxations was studied using participation ratios and effective masses. We found that participation ratios and jump lengths increase with increasing temperature. The structure of the relaxations was quantified by the dimensionality of the jumps. At low temperatures the relaxations consist of chains of atoms that are mainly one-dimensional. The dimensionality of the jumps increases with the temperature due to side branching of the chains. There exists a wide distribution of correlations between successive jumps at low temperatures. On increasing the temperature, we found very high and very low correlated jumps becoming rare. The former fact is due the sharp drop in the potential energy occurring during relaxations making reversible jumps to become rare events. The latter is due to the aggregations of various active regions to form large complexes. Analysis of the heterogeneity in the relaxations occurring in these systems was performed by the van Hove correlation function and the non-Gaussianity parameter. The van Hove correlation function especially for the O atoms exhibits peaks, which are characteristic for hopping processes. The analysis of non-Gaussianity parameters shows that the oxygen atoms probe a more heterogeneous environment than the silicon atoms and probably attributed to the smaller mass of oxygen atoms. For a longer time scale at low temperature (2000 K) the dynamics becomes more heterogeneous than at the higher one (3000 K). Caging effects are also found to be more prominent at lower temperatures.

**Acknowledgment.** Funding by the Deutsche Forschungsgemeinschaft through the SFB 408 is gratefully acknowledged.

## References and Notes

(1) Frick, B.; Richter, D. *Science* **1995**, *267*, 1939.
(2) Scott, W. W.; McCrone, R. K. *Phys. Rev. B* **1970**, *1*, 3515.
(3) Topp, K. A.; Cahill, D. G. *Z. Phys. B* **1996**, *101*, 235.
(4) Buchenau, U.; Zhou, H. M.; Nücker, N.; Gilroy, K. S.; Phillips, W. A. *Phys. Rev. Lett.* **1988**, *60*, 1318.
(5) Ediger, M. D.; Angell, C. A.; Nagel, S. R. *J. Phys. Chem.* **1996**, *100*, 13200.
(6) Böhmer, R.; Ngai, K. L.; Angell, C. A.; Plazek, D. J. *J. Chem. Phys.* **1993**, *99*, 4201.
(7) Goldstein, M. *J. Chem. Phys.* **1969**, *51*, 3728.
(8) Stillinger, F. H.; Weber, T. A. *Phys. Rev. A* **1983**, *28*, 2408.
(9) Malek, R.; Mousseau, N. *Phys. Rev. E* **2000**, *62*, 7723.
(10) Buchenau, U. *Phys. Rev. B* **2001**, *63*, 104203.
(11) Oligschleger, C.; Schober, H. R. *Phys. Rev. B* **1999**, *59*, 811.
(12) Büchner, S.; Heuer, A. *Phys. Rev. E* **1999**, *50*, 6507.
(13) Heuer, A.; Silbey, R. J. *Phys. Rev. Lett.* **1993**, *70*, 3911.
(14) Götze, W.; Sjögren, L. *Rep. Prog. Phys.* **1992**, *55*, 241.
(15) Brodin, A.; Börjesson, L.; Engberg, D.; Torell, L. M.; Sokolov, A. P. *Phys. Rev. B* **1996**, *53*, 11511.

(16) Caprion, D.; Matsui, J.; Schober, H. R. *Phys. Rev. Lett.* **2000**, *85*, 4293.
(17) Zorn, R. *J. Phys.: Condens. Matter* **2003**, *15*, R1025.
(18) Richert, R. *J. Phys.: Condens. Matter* **2002**, *14*, R703.
(19) Heuer, A.; Spiess, H. W. *Phys. Rev. Lett.* **1999**, *82*, 1335.
(20) Arbe, A.; Colmenero, J.; Monkenbusch, M.; Richert, D. *Phys. Rev. Lett.* **1998**, *81*, 590.
(21) Caprion, D.; Schober, H. R. *Phys. Rev. B* **2000**, *62*, 3709.
(22) Horbach, J.; Kob, W. *Phys. Rev. B* **1999**, *60*, 3169.
(23) Karpov, V. G.; Klinger, M. I.; Ignatiev, F. N. *Sov. Phys. JETP* **1983**, *57*, 439.
(24) Buchenau, U.; Galperin, Yu. M.; Gurevich, V. L.; Schober, H. R. *Phys. Rev. B* **1991**, *43*, 5039.
(25) Buchenau, U.; Galperin, Yu. M.; Gurevich, V. L.; Parshin, D. A.; Ramos, M. A.; Schober, H. R. *Phys. Rev. B* **1992**, *46*, 2798.
(26) Sanyal, S.; Sood, A. K. *Europhys. Lett.* **1996**, *34*, 361.
(27) Donati, C.; Douglas, J. F.; Kob, W.; Plimpton, S. J.; Poole, P. H.; Glotzev, S. C. *Phys. Rev. Lett.* **1998**, *80*, 2338.
(28) Oligschleger, C.; Schober, H. R. *Solid State Commun.* **1995**, *93*, 1031.
(29) Mukhopadhyay, A. B.; Oligschleger, C.; Dolg, M. *Phys. Rev. B* **2003**, *67*, 14106.
(30) Mukhopadhyay, A. B.; Oligschleger, C.; Dolg, M. *Phys. Rev. B* **2003**, *68*, 24205.
(31) Mukhopadhyay, A. B.; Oligschleger, C.; Dolg, M. *Phys. Rev. B* **2004**, *69*, 12202.
(32) Mukhopadhyay, A. B.; Dolg, M.; Oligschleger, C. *J. Chem. Phys.* **2004**, *120*, 8734.
(33) Nicolaides, C. P. *Appl. Catal., A* **1999**, *185*, 211.
(34) Kramer, G. J.; de Man, A. J. M.; van Santen, R. A. *J. Am. Chem. Soc.* **1991**, *113*, 6435.
(35) Olson, D. H.; Kokotailo, G. T.; Lawton, S. L.; Meier, W. M. *J. Phys. Chem.* **1981**, *85*, 2238.
(36) Schober, H. R.; Laird, B. B. *Phys. Rev. B* **1991**, *44*, 6746.
(37) Fletcher, R.; Reeves, C. M. *Comput. J.* **1977**, *26*, 339.
(38) Greaves, G. N.; Meneau, F.; Sapelkin, A.; Colyer, L. M., ap Gwynn, I.; Wade, S.; Sankar, G. *Nature Mater.* **2003**, *2*, 622.
(39) Greaves, G. N.; Meneau, F.; Sankar, G. *Nucl. Instrum. Methods Phys. Res. B* **2003**, *199*, 98.
(40) Oligschleger, C. *Phys. Rev. B* **1999**, *60*, 3182.
(41) Kob, W.; Andersen, H. C. *Phys. Rev. E* **1995**, *51*, 4626.
(42) Ngai, K. L.; Habasaki, J.; Hiwatari, Y.; León, C. *J. Phys.: Condens. Matter* **2003**, *15*, S1607.